

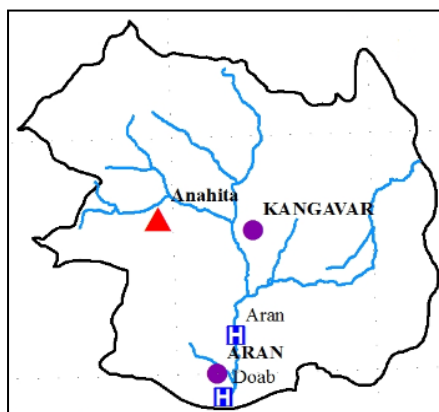
Prediction of SAR and TDS parameters using LSTM- RNN model: A case study on Aran station, Iran

Maryam Hafezparast Mavadat^{*}, Seiran Marabi^{*}

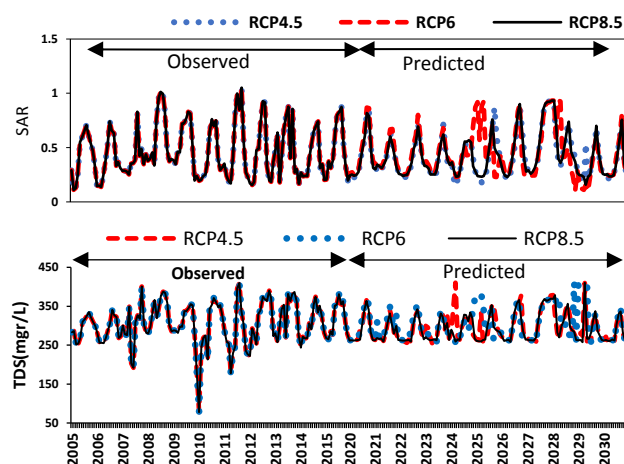
Department of Water Engineering, Faculty of Agricultural Science and Engineering, Razi University, Kermanshah, Iran.

GRAPHICAL ABSTRACT

Download precipitation and temperature from general circulation models



Water quality prediction with (LSTM)



ARTICLE INFO

Article history:

Received 1 June 2021

Reviewed 25 August 2021

Received in revised form 30 September 2021

Accepted 2 October 2021

Available online 3 October 2021

Keywords:

CMIP5 Scenarios

SAR

TDS

Rainfall-runoff

Prediction

LSTM-RNN

Article type: Research Article



© The Author (s)

Publisher: Razi University

ABSTRACT

Surface water quality is of particular importance due to its drinking, industrial, and agricultural water sources. Changes in rainfall, temperature and river discharge can affect surface water quality. In this study, the effect of CANESM2, FIO, GFDL, MIROC climate models and weight composition model of CMIP5 (Coupled Model Intercomparison Project) under representative concentration pathways (RCP) of 4.5, 6, 8.5 scenarios on rainfall and temperature were investigated and then monthly discharge of the Aran river in Iran during 2020-2052 and 2053-2085 is predicted using the IHACRES runoff model. Next, the LSTM (Long Short-Term Memory network)-RNN (Recurrent Neural Networks) model were used to predict the total dissolved solids (TDS), sodium adsorption ratio (SAR) for the period 2020-2030. The results showed that the long-term monthly rainfall under the RCP8.5 scenario reported a further decrease compared to the RCP4.5 and RCP6, and the rainfall fluctuations were higher than the other two scenarios. Temperature changes in the second period are higher than the first period, so that in the first period under the scenarios of RCP4.5, RCP6 and RCP8.5 showed respectively 1, 1.5 and 2 degrees Celsius increase, while in the second period, 2, 3 and 4 degrees Celsius is predicted. The average discharge shows by 15.8 % and 20.97 % respectively decrease under the RCP4.5 scenario in the first and second periods, while by 8.51 % and 27.55 % under the RCP6 scenario and 6.38 % and 39.89 % under the RCP8.5 scenario compared to the observed discharge. The mean, maximum, and minimum TDS parameters under RCP4.5 scenario are, respectively, 295, 410, and 263, and 302, 410, and 257 under RCP6 scenario while 292, 410, and 257 mg, for RCP8.5 scenario. These changes are, respectively, 0.42, 0.93 and 0.14 for the SAR parameter in RCP4.5 scenario, and equal to 0.44, 0.94 and 0.1 in scenario 6, while 0.42, 0.93 and 0.15, respectively, for RCP8.5 scenario in Khorramrood river.

1. Introduction

The intensification of human activities such as industrialization, land use change and urbanization create increasing pressure on the quality of surface water bodies (Delpla et al. 2009; Vörösmarty et al. 2010).

*Corresponding author Email: m.hafezparast@razi.ac.ir

Since surface water is an important resource in drinking water production, reducing water quality could negatively affect the production of safe drinking water. Therefore, an increasing variety and level of chemical and microbial contaminants is discovered in freshwater systems all around the world (Adjei. 2014; Baken et al. 2018;

Bunke et al. 2019; Kasmaei et al. 2016; Lapworth et al. 2018; Maier and Dandy. 1996; Roholamin Owusu-Boateng and Sluis. 2019). The effect of climate change on the biodiversity of freshwater has been studied and simulated in the world using paired models of climate change-hydrology and ecology. Climate change could change the regime of water resources, and some species expand their habitat in water resources and, in contrast, some species restrict their territory (Azari et al. 2013; Taei Semiromi et al. 2014; Tisseuil et al. 2012). Since water quality is affected by many factors and some of these factors have a complex nonlinear relationship, different methods of single and multivariate linear and nonlinear regression and artificial intelligence methods such as artificial neural network models can be used to obtain unregistered values. Regression models are highly consistent with data from out-of-range data, lost data, and data recorded irregularly (Ansari-pour et al. 2011). Recently, with the development of software techniques, modeling has been used as a powerful tool in various areas of water engineering (Azamathulla et al. 2008; Azamathulla. 2013). Researchers have tried to use these softwares to model water quality issues (Noori et al. 2015; Parsaie et al. 2015; Zare Abyaneh. 2014). The use of soft computing techniques such as neural network, adaptive neuro-fuzzy inference systems (ANFIS), genetic programming (GP), support vector machine (SVM), has led to high accuracy in water quality prediction. (Burchard-Levine et al. 2014; Chang et al. 2014; Cordoba et al. 2014; Nasr and Zahran. 2014; Van Ael et al. 2015). Nikoo et al. (2011) studied the water quality of the Karun river, the largest river in the Iran, using parameters measured at existing stations along the river (Shahid Abbaspour-Arab Assad Basin). The sodium adsorption ratio (SAR) and total dissolved solids (TDS) measured using the neural network model were also predicted at the same stations. The results showed that the selected artificial neural network model has more ability, flexibility and accuracy in predicting river water quality than nonlinear regression statistical models. Palani et al. (2008) used neural networks to predict the qualitative characteristics of Singapore's coastal waters. Rajaei and Mirbagheri. (2009) have also used neural networks to predict the suspended load of rivers. Noushadi et al. (2008) simulated some water quality parameters of Zayandehrud river in Iran including electrical conductivity (EC), total dissolved solids (TDS), acidity, bicarbonate, and chloride using neural network. This model was able to provide reliable results for predicting these parameters. Gazzaz et al. (2012) used multilayer perceptrons (MLPs) neural networks to estimate the water quality index of the Kinta river in Malaysia. The results showed that the neural network model could be a good alternative to long-term calculations of water quality index. Given the importance of the sodium adsorption ratio (SAR) for plants growing, it is essential to predict water quality management for irrigation. Asadollahfardi (2013) modeled the sodium adsorption ratio (SAR) using artificial neural network for Chal Ghazi river in Kurdistan, northwestern Iran. The study used a multilayered perceptron neural network (MLP) and average monthly data for the period 1998-1999. The input parameters to the MLP network are discharge, sulfate, sodium, calcium, chloride, magnesium and bicarbonate, and the output of the sodium adsorption ratio is predicted by the model. The results showed that the correlation coefficient of 0.976 between the actual and predicted values of SAR means that the accuracy of the model is acceptable. Ansari-pour et al. (2001) Studied artificial neural network models and multivariate regression to predict water quality parameters in Sefidrood river in Iran. For this purpose, the time series of discharge and quality parameters of electrical conductivity, bicarbonate, chlorine, sulfate, acidity, sodium, potassium, calcium, magnesium and total dissolved solids during 1982-2005 were used from Astaneh hydrometric station. Simulation and prediction of these parameters showed that the neural network has a higher capability than multivariate regression in this field. Salami et al. (2016) used two methods of mathematical modeling and artificial neural network to simulate and predict the qualitative characteristics of river water such as: dissolved oxygen (DO), total dissolved solids (TDS), total hardness (TH), alkalinity (PH), turbidity (TU), conductivity electric (EC), temperature (T), acidity (PH) were used. Apart from alkalinity, all water quality parameters in the neural network model had a coefficient of determination close to 0.99 while the neural network model to simulate alkalinity with coefficient of determination of 0.82. According to the water quality changes under climate scenarios, Shahkarami (2018) analyzed the trend in water quality components at Tire river Doab station in Iran for a period of 15 years using statistical tests during spring and winter. The test indicated a significant trend at 90 % confidence level for K, Na, Mg, Ca, SO₄, Cl and HCO₃. EC increased in spring and indicated significant trend at a 95 % confidence level in winter. Total dissolved solids (TDS) represented the 95 % significant confidence level. The results showed the potential effects of global climate change on declining water quality. Baek et al. (2020) combined neural network

(CNN) - long short-term memory (LSTM) was created with a deep learning approach by combining CNN and LSTM networks with simulated water quality including total nitrogen, total phosphorus and total organic carbon. This study revealed that the performances of both of the CNN and LSTM models were effective with above the Nash-Sutcliffe efficiency value of 0.75 and that those models well represented the temporal variations of the pollutants in Nakdong river basin in Korea. Traditional forecasting methods have lots of problems, such as low accuracy, poor generalization, and high time complexity. In order to solve these shortcomings, a novel water quality prediction method based on the deep LSTM learning network is proposed to predict pH and water temperature. It is predicted based on LSTM and constructed using the preprocessed data and its correlation information. Results show that, in the short-term prediction, the accuracy of pH and water temperature can reach 98.56 % and 98.97 % (Hu et al. 2019).

According to the Intergovernmental Panel on Climate Change (IPCC), the main elements in climate conditions that affect the quality of surface water and drinking water are temperature, rainfall and droughts (Jiménez Cisneros et al. 2014). Increase in temperature affects almost all the physicochemical equilibria and biological reactions, and more frequent extreme hydrological events change the concentration of chemicals or pathogenic microorganisms in the aquatic ecosystems (Delpla et al. 2009; Sluis. 2019; Whitehead et al. 2009). Bal et al. (2016) studied climate change effects on water quality in Yamaha river in U.S.A. Finally, the developed qualitative model used to improve the predictive power and provide information for the decision-making process. Slaughter et al. (2016) studied the quality of Olifants river catchment in South Africa in terms of nutrients (sodium, phosphate, etc.) and the electrical conductivity (EC). The model was calibrated during the observation period 1999-2005. Then, the qualitative status of the river over the period 2046-2065 was simulated using the calibrated model and forecasted by climatic scenarios of the IPCC fourth assessment report (AR4). The results show the slight increase in dilution and nutrient input. Hosseini et al. (2017) examined the impact of climate change on the quality of Prairie Regulated river that the results indicated the flow of the Qu Appelle river in Canada which is used to meet the needs of agriculture, industry and population growth in southern Saskatchewan has increased. Due to an increase in discharge and temperature because of climate change, it is expected that changes in these factors will affect the quality of river water. A qualitative model, a water quality analysis simulation program (WASP), was used to simulate current and future river water quality. Then, the model was used to predict water quality (nutrient concentration and dissolved oxygen) during the period of 2050-2055 and 2080-2085. The results of the modeling show that rising water temperature could increase the amount of ammonium and nitrate while decrease the dissolved oxygen and orthophosphate in summer. Mukundan et al. (2020) studied the effect of climate change on nutrient loading in the Cannonsville Reservoir watershed, New York. They calibrated a modified version of the SWAT model entitled the SWAT-Hillslope model (SWAT-HS) to evaluate the contribution of nitrate from point and nonpoint sources. Eghtetaf et al. (2015) aimed to investigate the effects of climate change on rainfall, temperature, runoff and surface water quality parameters in Baleqlu Chai river basin located in Ardabil province using LARS - WG downscaling model ,HADCM3 model outputs, under scenario A2 surveyed the Baleqlu Chai basin for three time periods (2011-2030, 2046-2065 and 2080-2099). The results show a 5°C rise in temperature and a decrease in the average annual rainfall to 14 mm during the 2080 to 2099 period. Using the parameters of temperature, precipitation and runoff and neural network model, changes in TDS and EC values, which are considered respectively as important parameters of water quality for drinking and agriculture, were estimated under climate change conditions. The results show an increase (3 %) in each of the above parameters. That surface water quality simulations have been performed using artificial neural network models in different parts of the world and have had satisfactory results. As far as previous researches have been studied, LSTM-RNN algorithm has not been used to predict TDS and SAR in climatic conditions. Due to the extensive advancement of deep learning in neural network and the capabilities of Python programming language with Keras, Torch and Tensor flow libraries in analyzing and predicting the time series, the innovation of this research is in using this algorithm using Keras library in predicting the qualitative parameters of TDS and SAR under the climatic scenarios of the fifth report.

2. Materials and methods

In recent decades, due to the industrialization of human societies and the increase in greenhouse gases, the effects of climate change on

temperature, precipitation and river discharge have been considered. In particular, fluctuations in the discharge time series, droughts and wet years have affected the quality of surface and groundwater. In this study, TDS and SAR changes caused by climate change in Aran station are predicted and the steps of the research process are shown in Fig. 1.

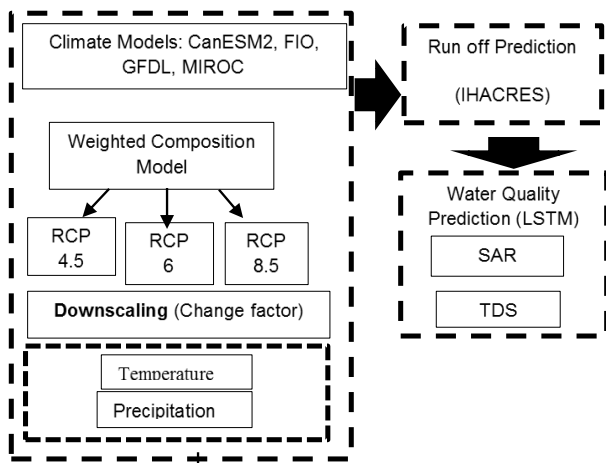


Fig.1. Research structure diagram.

2.1. Study area

The study area is located in the east of Kermanshah province, Khorramrood river basin, Kangavar city which has an area of about 674 square kilometers and one of the most important places for horticulture and agriculture. In this region, the majority of rain falls during December and January. A large part of western Iran is formed by high and interconnected Zagros heights, and the fertile plain of Kangavar in the west of Zagros Mountains is situated at an altitude of 1457 meters above sea level. The heights of the Middle Zagros has covered the northern and northwestern parts of this vast plain. Water in Kangavar fertile plain is supplied by receiving good rainfall that is stored in aquifers or from the many mirages of this region, which is formed in

Khorramrood, Asadabad and Kangavar rivers and the confluence of these rivers create Gamasiab river. The present study examines the effects of climate change on the Khorramrood river discharge of the Aran base station, which is located at 47.925 degrees east longitude and 34.41 degrees north latitude. The Khorramrud river originates from the southeastern highlands of Malayer city and joins Gamasiab river in the provinces of Hamadan and Kermanshah Fig. 2.

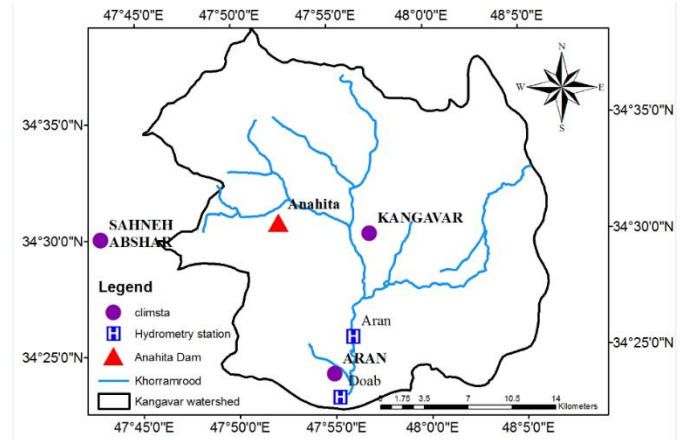


Fig. 2. Kangavar watershed.

2.2. Weather data, water quality and quantity

Monthly quantitative and qualitative data of Khorramrood river including flow discharge, main cations and anions (calcium, magnesium, sodium, sulfate, chloride and carbonate), total dissolved solids (TDS), electrical conductivity (EC), the sodium adsorption ratio (SAR), PH and monthly historical weather data (temperature and rainfall) are obtained from Aran hydrometric station and Kangavar synoptic station during the 1983-2015 period from Kermanshah meteorological organization and Regional Water Company of Kermanshah (Tables 1 and 2).

Table 1. Weather data of Kangavar synoptic station and river runoff in Khorramrood river.

Month	Jan	Feb	Mar	Apr	May	Jun	Jul	Aug	Sep	Oct	Nov	Dec
Mean	58	65	69	53	36	4	1	1	3	28	67	63
Max	283	305	339	108	211	21	8	13	19	83	347	176
Min	13	27	22	0	5	0	0	0	0	0	11	0
Mean	-0.06	2.3	6.97	2.96	16.85	22.53	26.5	25.8	20.76	14.8	12.08	7.78
Max	4.47	6.87	11.0	7.28	20.06	25.87	29.8	28.3	23.89	17.6	15.41	10.87
Min	-8.65	-8.30	1.46	-1.2	13.7	18.6	23.4	22.2	17.97	12.8	9.9	5.5
Mean	5.23	6.53	8.2	8.2	5.31	1.81	0.30	0.06	0.05	0.51	2.92	5.00

Table 2. Water quality parameters of Khorramrood river

Parameter	Na, meq/L	Ca, meq/L	Cl, meq/L	Mg, meq/L	TDS, meq/L	EC, moh/cm	So ₄ , meq/L	pH	TH	Water temperature °C
Mean	0.75	2.54	0.59	1.47	298	464	0.57	7.9	230	13.2

2.3. Climate models

In order to generate climate scenarios for the future periods 2020-2052 and 2053-2085, the output of 4 models of the IPCC Fifth Assessment Report (AR5) that were more consistent with the historical data of this region including FIO (128*64), GFDL (144*90), MIROC (128*64) under scenarios RCP4.5, RCP6 and RCP8.5 and the CanESM2 (128*64) model are used under RCP4.5 and RCP8.5 scenarios. The CanESM2 does not have an RCP6 scenario.

2.4. The weighting method of mean observed temperature-precipitation (MOTP)

Since the output of each climate model includes uncertainty so it is better to choose climate models that have had similar results in the historic period in the studied area, and in order to reduce the uncertainty of each model, the AR5 models could be weighted using MOTP method based on the standard deviation of the mean temperature or simulated rainfall for the baseline period from the average observed data according to Eq. 1.

$$W_{ij} = \frac{\frac{1}{\Delta P_{ij}}}{\sum_{i=1}^N \left(\frac{1}{\Delta P_{ij}}\right)} \quad (1)$$

where, W_{ij} is the weight of GCM_j in month i ; and ΔP_{ij} is the difference between average temperature or precipitation simulated by GCM_j in month i of base period and the corresponding observed value (Massah Bavani. 2006).

2.5. Downscaling

The Delta method has been widely used in studies of atmospheric general circulation models to assist climate change studies. For the precipitation, the delta factor is obtained by dividing the model evaluation value by the historical value of the model and the change factor obtained for the precipitation parameter is multiplied by the time series of the precipitation. This function is performed in any time from annual to monthly and the use of a monthly scale prepares the seasonal assessment (Guilbert. 2016). The change factor method, because of its simplicity, has a popular approach to analyzing climate change (Diaz-Nieto and Wilby. 2005; Déqué et al. 2007; Prudhomme et al. 2002). In this method, the basic assumption is that relative changes in climate models are more reliable than absolute values (Ntegeka et al. 2014). Relationships 2 to 5 show how to apply this factor on precipitation and temperature data. In order to downscale the data locally, a proportional method is used that AOGCM simulated climatic variables are extracted from cellular information which the target area is located in.

$$\Delta T = \bar{T}_{AOGCM,Fut,i} - \bar{T}_{AOGCM,Base,i} \quad (2)$$

$$\Delta P_i = \left(\frac{\bar{P}_{AOGCM,Fut,i}}{\bar{P}_{AOGCM,Base,i}} \right) \quad (3)$$

$$T = T_{Obs} + \Delta T \quad (4)$$

$$P = P_{Obs} \times \Delta P \quad (5)$$

In Eq. 2, ΔT_i is climate change scenario of 33-year long-term average temperature for each month; $\bar{T}_{AOGCM,Fut,i}$ is the average 33-year temperature simulated by each AOGCM model in the future period for each month, $\bar{T}_{AOGCM,Base,i}$ is average temperature simulated by each AOGCM model in the observation period for each month. In Eq. 3, the above is true for rainfall. In Eq. 4, T is the time series resulting from the climate scenario of temperature for the future period, T_{obs} is the time series of observed temperature in the base period (1983-2015), and ΔT is the temperature change. For rainfall, the cases mentioned in Eq. 5 are also established.

2.6. IHACRES rainfall runoff model

Three popular and widely-used conceptual rainfall-runoff models were chosen (Andréassian et al. 2012; Shin et al. 2016; Van Werkhoven et al. 2009). These three models have different structures. First, The GR4J model (Perrin et al. 2003) is considered as a daily lumped conceptual rainfall-runoff model which has four parameters, two stores (production and routing stores) and two unit hydrographs. Second, the IHACRES rainfall-runoff model that is proposed by Jakeman and Homberger. (1993) explains the basin hydrological behavior well in the event that the surface water is the principal component of the flow regime. This is a simple model designed to do the hydrograph identification and component flows from rainfall, evaporation, and stream flow data. In this model the rainfall-runoff processes are illustrated using two modules. Third, the Sacramento model (Burnash et al.1973) parameterize soil moisture distribution at different depths of interconnected soil tanks including five runoff components: direct runoff originating from impervious area, surface runoff, interflow, supplementary base flow, and primary base flow. In this study, the IHACRES semi-conceptual rainfall-runoff model was used to produce monthly runoff and the study on variations of climatic parameters on runoff was performed in different climate scenarios for the next two periods 2020-2052 and 2053-2085.

2.7. Water quality model

In this study, as it is difficult to access surface water quality data due to the weakness of databases. The sodium adsorption ratio (SAR) and total dissolved solids (TDS) which had more complete data, was considered. In order to fix incomplete data, the information of Doab hydrometric station, which is located downstream of the study station and also the information of company, which has been active in the study area was used. A ten-year monthly time series was arranged from 2005-2015 for these two qualitative parameters. Eight years of this data is considered for training and two years for testing. The TDS and SAR monthly time series are shown in Fig. 3. Hind et al. (2018) checked that previous studies have used different neural network (ANN) models to forecast TDS (Asadollahfardi et al. 2011; Asadollahfardi et al. 2017; Ghavidel and Montaseri. 2014; Kalin et al. 2010; Najah et al. 2013), So the power of LSTM can be utilized. LSTM is a kind of artificial recurrent neural network used to learn long term dependencies and remember the past information also while predicting the future values, takes this past information into account (Hochreiter and Schmidhuber. 1997). This model has been developed for different climate scenarios using Python programming language and LSTM method and Keras Deep Learning Library. The steps for normalizing data and dividing data for steps of training, testing and formation of the LSTM model are summarized as follows.

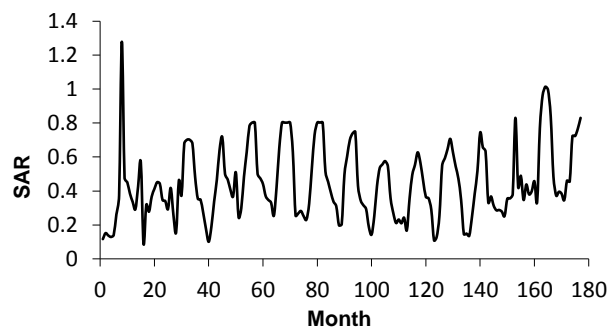
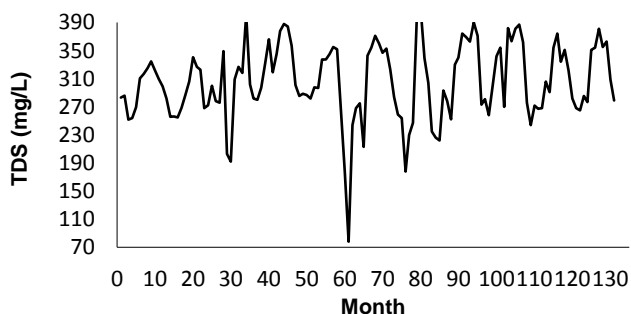


Fig. 3. Monthly observed TDS and SAR.

2.8. Creating LSTM model

LSTM is able to remove and add information to the cell arranged by a structure named a gate. The first step in the LSTM is to decide what kind of information is going to remove from the cell. This decision has been made by the sigmoid layer called the layer of forget gate, where h_{t-1} and x_t . h_{t-1} is the output value of the previous layer and x_t is the input value that will enter the layer. The forget gate function is expressed as a function f_t which can be written as Eq. 6 (Puriyanto et al. 2019).

$$f_t = ([h_{t-1}, x_t] + b_f) \quad (6)$$

The next step is to decide what kind of information is going to store in the cell. First, the sigmoid layer is named the input gate layer while decide which value to update is written as i_t , tanh layer will create a vector of the new candidate value that is written as C_t , both will be combined to update the cell. The functions i_t and C_t could be written in the following Eq. 7 (Puriyanto et al. 2019).

$$\begin{aligned} i_t &= ([h_{t-1}, x_t] + b_i) \\ C_t &= \tanh(WC[h_{t-1}, x_t] + b_c) \end{aligned} \quad (7)$$

The next step would be to update the old cell value C_{t-1} to the new cell value C_t . The function C_t can be written as the Eq. 8.

$$C_t = f_t \times C_{t-1} + i_t \times C_t \quad (8)$$

The final step is to decide which information will be released. The output will be based on cell but filtering needs to be done. First, run on the sigmoid layer which decides which part of the cell to output is written as o_t . Next, enter the cell past the $\tanh(C_t)$ and multiply it by o_t written as h_t . Functions o_t and h_t can be expressed in Eq. 9.

$$\begin{aligned} o_t &= ([h_{t-1}, x_t] + b_o) \\ h_t &= o_t \times \tanh(C_t) \end{aligned} \quad (9)$$

where, x_t = input; h_t = hidden state; c_t = cell state; f = forget gate; g = memory cell; i = input gate; o = output gate... W_f, W_c, W_i, W_o called weight and b_f, b_c, b_i, b_o called bias that are obtaining in training and testing process. σ is the sigmoid activation function. The architecture of LSTM for the regression purpose can be seen in Fig. 4.

2.9. Data normalization

Going by the rule of thumb, whenever a neural network is used, the data should be normalized or scaled. For this purpose Min_ Max_ Scaler class from the Sklearn_preprocessing library would be used to scale the data between 0 and 1. Meanwhile, the feature_range parameter is applied to determine the range of the scaled data parameter (Hind et al. 2018). The data has been preprocessed and it is divided into training and test sets by train_test_split method of Scikit learn. A class LSTM (from keras.layers imported LSTM) defined and comprised of multiple layers. LSTM layers added to the model along with a dense layer that predicts the future TDS parameter (Hind et al. 2018).The LSTM algorithm trained on the training set. Next, the model used to predict on the test set. The resulting predictions compared with the actual values of the test set to measure the trained model performance.

2.10. Accuracy assessment

In order to evaluate the predictive performance of the IHACRES and LSTM-RNN models, three performance measures have been used. The performance measures in Eqs. 10-12 show the accuracy of model's predictions by comparing the actual parameter's value (F_t) and

the simulated value (A_t) for sample t , and the number of samples (N) was included in some of the measures to get normalized values, which could be useful when comparing different models. Firstly, Root Means Squared Error (RMSE) was used to evaluate the average performance of the model among different testing samples. Mean Absolute Error (MAE) estimates the average magnitude of the errors in a set of forecasts aside from their direction. It evaluates accuracy for consecutive variables.

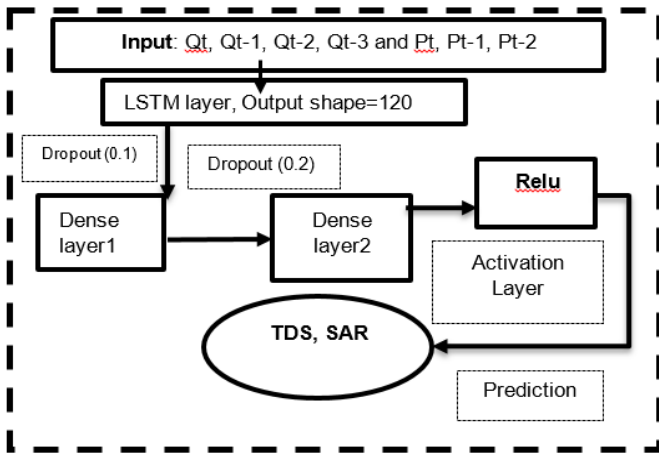


Fig. 4. The RNN model proposed for predicting TDS and SAR.

MAE is the arithmetic average over the verification sample of the absolute values of the differences among the forecast and the corresponding observation. The coefficient of Determination (R^2) was used to estimate the correlation between observation and simulation (Asadollahfardi et al. 2017).

$$RMSE = \sqrt{\frac{1}{N} \sum_{t=1}^N (A_t - F_t)^2} \tag{10}$$

$$MAE = \frac{1}{N} \sum_{t=1}^N |A_t - F_t| \tag{11}$$

$$R^2 = 1 - \frac{\sum_{t=1}^N (A_t - F_t)^2}{\sum_{t=1}^N (A_t - A)^2} \tag{12}$$

where, N is the number of data; A_t is the actual value of data and F_t is the predicted data (Hind et al. 2018).

3. Results and discussion

Table 3. Increasing and decreasing changes of precipitation in climate models by season.

Scenario	Time	First duration (2020-2052)					Second duration (2053-2085)				
		Model	CanESM2	FIO	GFDL	MIROC	Weighted model	CanESM2	FIO	GFDL	MIROC
RCP 4.5	Winter	2.96	-12.60	1.55	1.75	-3.45	-3.47	-17.62	-4.83	-11.47	-8.60
	Spring	-2.14	-16.45	4.16	32.83	7.58	-3.03	-16.75	-4.58	17.43	-1.33
	Summer	43.36	18.55	16.19	10.41	15.88	7.59	-34.26	-59.75	-48.72	-35.31
	Autumn	16.70	-5.30	-20.69	-14.22	-6.39	40.45	-13.52	-46.40	-26.77	-6.40
RCP 6	Winter	-	-16.51	1.55	-11.61	-12.73	-	-17.62	-4.57	-23.77	-18.27
	Spring	-	-18.65	4.16	17.12	0.92	-	-16.75	-1.00	30.29	5.08
	Summer	-	77.34	16.19	-24.89	42.37	-	-34.26	-2.75	15.48	-18.36
	Autumn	-	12.15	-20.69	5.26	-4.81	-	-13.52	2.20	-7.82	-9.96
RCP 8.5	Winter	-11.92	-6.43	-23.81	1.25	-10.72	-3.88	-22.95	-29.61	-15.02	-19.04
	Spring	-33.02	-11.12	-30.32	17.28	-13.13	-29.94	-15.85	-29.47	20.04	-14.42
	Summer	147.91	-31.66	198.41	-15.51	58.41	136.03	-6.77	141.45	29.24	61.99
	Autumn	0.31	17.15	-26.64	1.11	-1.13	13.34	21.78	-26.80	21.10	7.35

*Negative values indicate the decrease whereas positive values show the increase

3.2. Changes in precipitation and temperature in weighted model

The weight combination model is considered to represent four climate models for each climate scenario as well as for each period in the future, and changes in the prediction of precipitation and temperature parameters with its observed value is shown in Fig.5. Meanwhile, Climate scenarios are considered as linear graphs and observed values are as columns. As the results of the three scenarios of the weight combination model show the long-term monthly rainfall under the RCP8.5 scenario reports a further decrease compared to RCP4.5 and RCP6. Also, rainfall fluctuations under RCP8.5 scenario are higher than the other two scenarios. The 2020 weight combination model predicts an upward trend compared to the basic period during the summer in all three scenarios while during the spring in the RCP4.5 and RCP6 scenarios. In other cases, decline in rainfall is expected. During the 2053, an increasing trend was predicted for RCP6 in spring season and for RCP8.5 in fall and summer and in the other cases, the

In this section, the results of this study including climate parameter forecasting, precipitation and temperature variations, runoff forecast with IHACRES model, TDS, SAR forecasts with artificial neural network model are shown respectively.

3.1. Prediction of climate parameters in future duration

The lowest decrease in precipitation is -1.33 in the spring of the 2053 period the weight combination model and the lowest increase in rainfall of +1.55 in the winter of the 2020 period is the GFDL-CM3 model. Winter rainfall in the CanESM2, GFDL-CM3 and MIROC-ESM-CHEM models increased in the 2020 period and decreased for the rest of it. In the RCP4.5 weight combination model, precipitation changes of -35.31 to 15.88 % are expected. Under the RCP6 scenario, precipitation changes is reported from 77.34 % in the fall during 2020 of the weight combination model to 34.26 % in the summer of the 2053 FIO-ESM model. In winter, all models, except the GFDL-CM3 in 2020, predict a downward trend for rain. The RCP6 weight combination model shows precipitation changes from +42.37 to -18.36. Rainfall changes under the RCP8.5 scenario was observed from +198.4 % in the spring of the 2020 of GFDL-CM3 model to -33.02 in the summer of the 2020 CanESM2 model. In the winter, all models except the MIROC-ESM-CHEM in the 2020 period, which has an increasing trend, are declining. Changes in precipitation of the weighted combination model have been reported from 61.99 % to 14.42 %. It can be seen that most of the climate models predict an increasing trend in the temperature parameter. Temperature changes compared to the observation period under the RCP4.5 scenario from +5.26 C in the summer 2053 by GFDL-CM3 model to -0.546C in the winter 2020 by FIO-ESM model is forecasted. The FIO-ESM model reported the lowest temperature decrease in all three scenarios. Temperature changes under the RCP6 scenario was observed from +4.63 C in the summer during 2053 using the GFDL-ESM2 model to +0.384. C in the winter 2053 by FIO-ESM model. Temperature changes under the RCP 8.5 scenario from +6.747 C in the fall 2053 by GFDL-CM3 model to -0.27C in the winter 2020 by 2CanESM model were reported, The GFDL-CM3 model predicts the highest temperature increase in all three scenarios. In the spring, summer and fall seasons, all models predict an upward trend. In winter, with the exception of the 2020 FIO-ESM models under the RCP4.5 scenario and the 2020 CanESM2 model under the RCP4.5 and RCP8.5 scenarios, the rest of the models report an upward trend for future temperatures. These parameters changes during different seasons of the year are shown in Tables 3 and 4.

changes in rainfall are decreasing. Decline in long-term average rainfall decrease for the 2053 period is higher than the 2020 period. Increasing temperature changes under the RCP8.5 scenario are much higher than the other scenarios, so that, in the first period under the scenarios of RCP4.5, RCP6 and RCP8.5, the temperature is increased respectively by 1, 1.5 and 2 °C whereas in the second period, the temperature raised of 2, 3 and 4 °C respectively.

3.3. Prediction of runoff with IHACRES model

IHACRES model is a catchment-scale rainfall – run off model whose purpose is to characterize the dynamic relationship between rainfall and stream flow, using rainfall and temperature (or potential evaporation) data, and to predict stream flow. It can be used to fill gaps in data, extend stream flow records, as well as explore the impact of climate change and identify effects of land use changes (Nazari-pooya et al. 2015).

Table 4. Increasing and decreasing changes of temperature in climate models by season.

Scenario	Time	First duration (2020-2052)					Second duration (2053-2085)				
		CanESM 2	FIO	GFDL	MIRO C	Weighted model	CanESM 2	FIO	GFDL	MIR OC	Weighted model
RCP 4.5	Winter	-0.378	-0.546	1.487	1.049	0.346	2.819	0.252	2.862	1.527	1.931
	Spring	0.453	0.186	1.725	1.254	0.943	2.660	1.009	3.451	2.606	2.491
	Summer	1.892	0.672	2.806	1.730	1.831	2.973	0.863	5.261	3.275	3.188
	Autumn	2.158	0.933	2.268	1.486	1.850	3.457	0.732	4.167	2.543	2.977
RCP 6	Winter	-	0.384	1.459	0.888	0.802	-	1.148	3.128	2.001	1.997
	Spring	-	0.780	1.740	1.113	1.843	-	1.209	3.147	2.231	2.813
	Summer	-	0.805	2.712	1.495	2.843	-	1.402	4.636	2.906	4.093
	Autumn	-	0.901	1.903	1.038	1.427	-	1.276	3.902	2.099	2.506
RCP 8.5	Winter	-0.377	0.729	2.572	1.360	1.013	4.244	1.841	4.453	2.861	3.435
	Spring	1.979	0.944	2.391	1.530	1.769	3.886	2.325	4.680	3.737	3.739
	Summer	2.112	1.468	3.050	2.210	2.241	4.758	2.995	6.747	4.616	4.883
	Autumn	2.579	1.691	2.730	1.528	2.268	5.416	2.753	6.237	3.676	4.807

*Negative values indicate the decrease whereas positive values show the increase

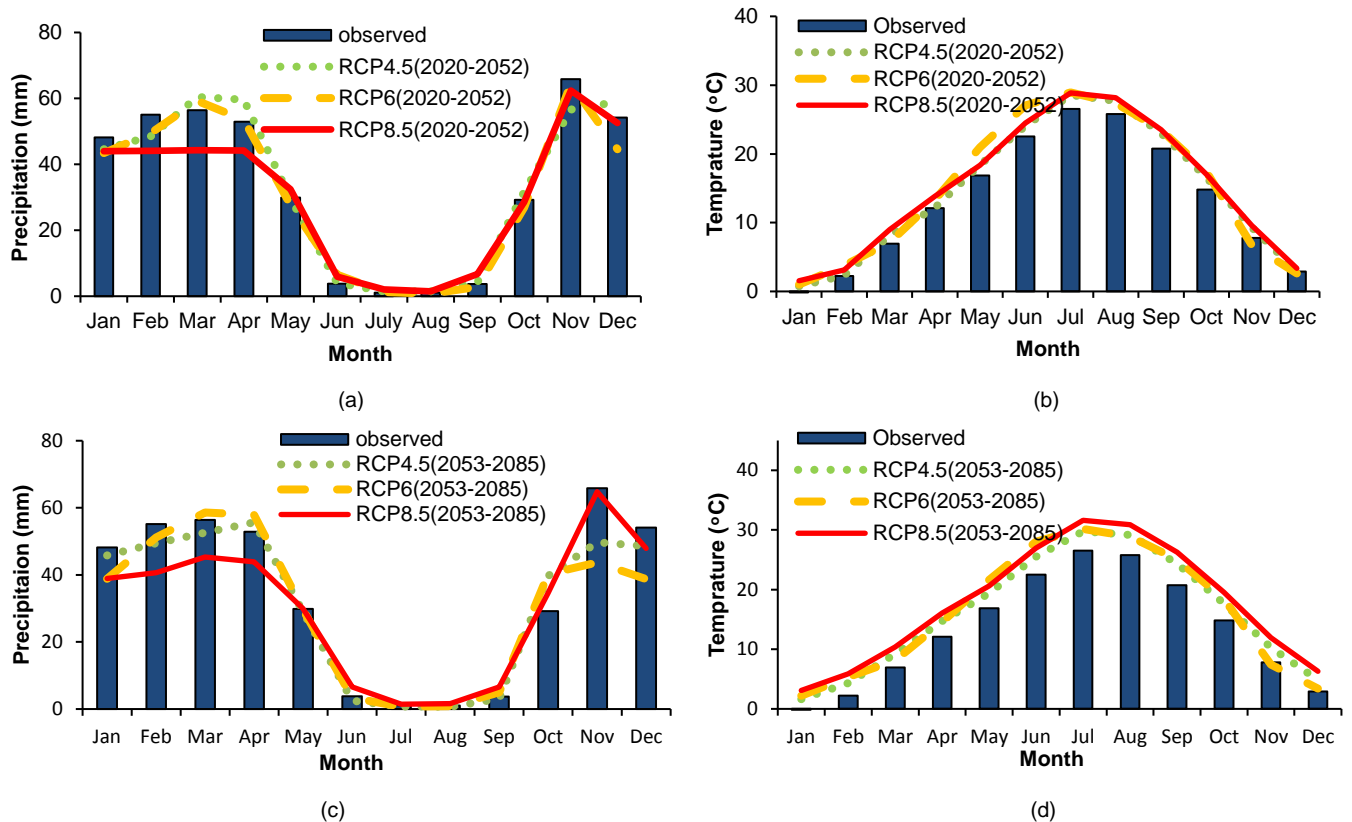


Fig. 5. (a) Predicted Rainfall with weighted model in different RCPs in (2020-2052); (b) Predicted Temperature with weighted model in different RCPs in (2020-2052); (c) Predicted Rainfall with weighted model in different RCPs in (2053-2085); (d) Predicted Temperature with weighted model in different RCPs in (2053-2085).

The important limitations are the need for a large amount of input data and the time required for model development, calibration, and simulation. As shown in Table 2, the average discharge of the Khorramrood river in the Aran station is 3.29 m³/s and the maximum and minimum discharge are 29.66 and 0.6 m³/s, respectively. In order to calibrate and validate the rainfall-runoff model of IHACRES, the monthly data of temperature, rainfall and discharge data during the 1983–2015 period were used. The calibration parameters of the IHACRES model are shown in Table 5. During this period, various years were tested to develop the model. The results showed that the period 1986/5 to 2004/10 with the correlation coefficient (R) and the error criteria presented in Table 6 had a good performance compared to the observation period. Therefore, these data were selected for the calibration and the rest of the data were considered for testing. After calibrating the rainfall-runoff model parameters, the rest of the data was used to validate the model. According to the calibration and validation results of the IHACRES model, the predicted values of discharge in climate models were performed and its comparison with the observational data is shown in Table 7. Under the RCP4.5 scenario, the average discharge value is 2.77 m³/s while the maximum predicted discharge is 24.95 m³/s and the minimum discharge is zero during the next period. In the second futures period, the average discharge is 2.6 m³/s whereas the maximum discharge is 29.5 m³/s and the minimum discharge of zero is predicted.

Table 5. IHACRES calibration parameters.

Parameter	Explanation	Parameter range	Optimum value
C	Humidity storage capacity	-	0.0021
T(W)	Drying time	1-30	1.02
F	Watershed temperature coefficient	0-4	3.2
I	Humidity threshold coefficient	0-0.5	0.02
P	Soil humidity intensity	1-3	1.03
a(s)	Drought Index	-	-0.188
B(s)	Peak index	-	2.15
T(s)	Slow down flow	-	0.616
V(s)	Volume ratio	-	2.9
Tref	Reference temperature	-	20

Table 6. Performance criteria in IHACRES model.

Performance criteria	R ²	RMSE	MAE	NSE	
IHACRES	Calibration	0.93	2.02	1.20	0.79
	Verification	0.80	3.24	2.29	0.68

Therefore, the average discharge in the first and second periods shows a decrease of 15.8 % and 20.97 %, respectively, compared to the observed discharge. Under the RCP6 scenario, the weight combination model during the next period has predicted the average discharge of 3.01 m³/s, the maximum discharge of 37.1 m³/s while the minimum discharge of zero for the Khorramrood river. The average, maximum and minimum discharge values are predicted respectively by 2.4, 24.05 and zero m³/s for the second future period. Therefore, the average discharge during the first and second period shows a decrease

of 8.51 and 27.05 percent, respectively, compared to the observed discharge. Under the RCP8.5 scenario, in the first future period, the average, maximum and minimum values of discharge were, respectively, 3.08, 26.68 and zero m³/s. In the second future period, these values are predicted of 2.8, 34.02 and zero m³/s, respectively. Therefore, the average discharge value for the first and second periods shows a decrease of 6.38 and 39.89 percent, respectively, compared to the observed discharge (Fig. 6).

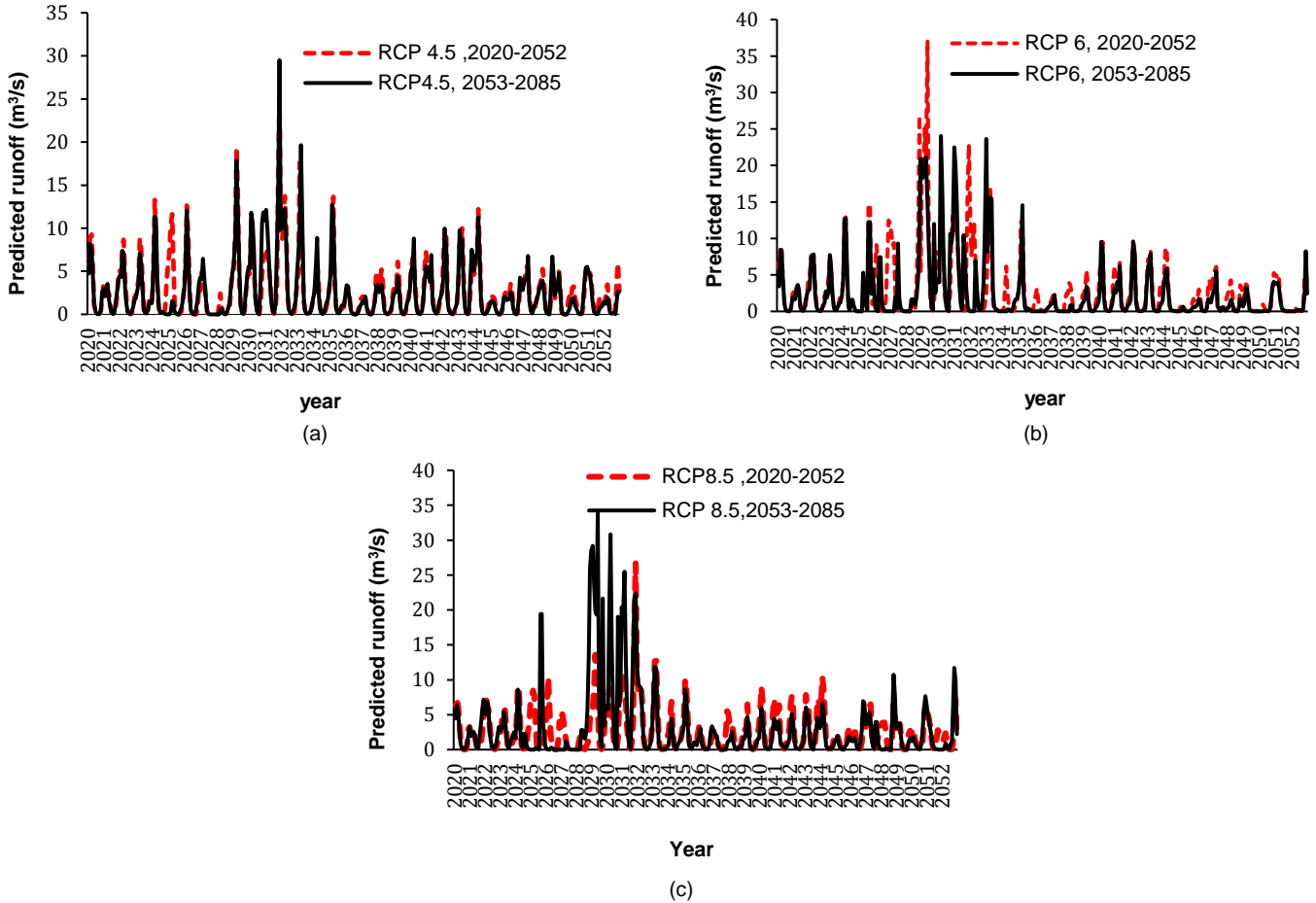
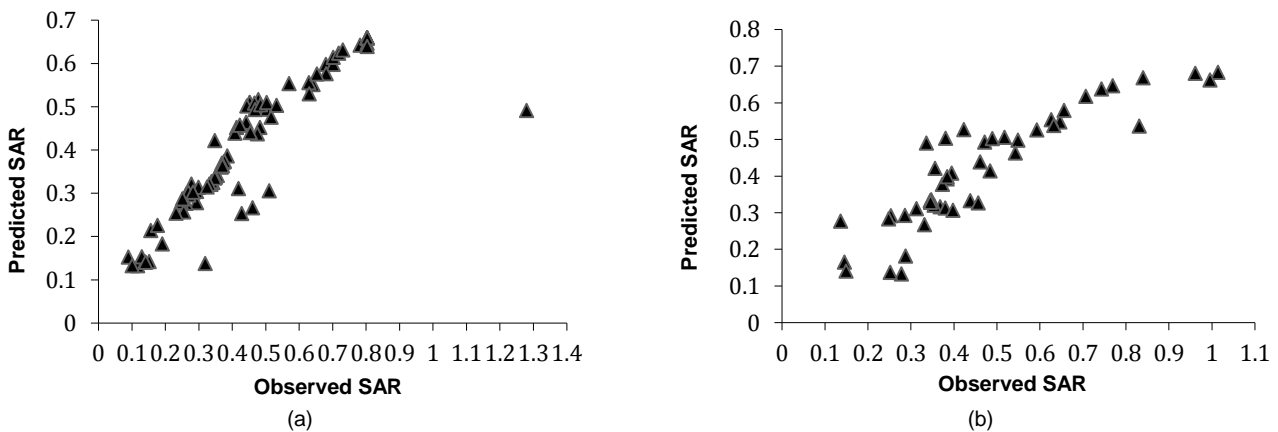


Fig. 6. Predicted runoff of weighted combination model in different RCPs.

Table 7. Comparing prediction and observation runoff (m³/s) in RCP scenarios.

RCP scenarios	Duration 2020-2052						Duration 2053-2085				
	Observed runoff	CanESM	FIO	GFDL	MIROC	Weighted combination model	CanESM	FIO	GFDL	MIROC	Weighted combination model
RCP 4.5		2.87	2.59	3.52	3.00	2.77	3.02	2.62	2.79	2.82	2.6
RCP 6	3.29	-	2.66	2.90	3.41	3.01	-	2.32	2.68	3.09	2.4
RCP 8.5		2.24	3.10	2.33	3.71	3.08	2.44	3.08	2.33	4.62	2.8



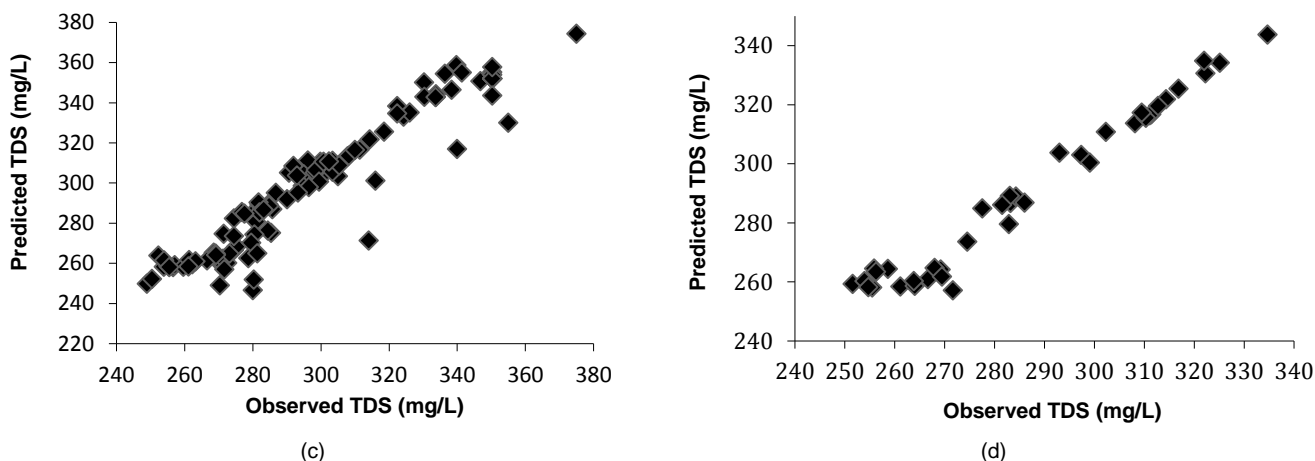


Fig. 7. (a) Observed and predicted SAR correlation in calibration duration in LSTM-RNN model; (b) Observed and predicted SAR correlation in verification duration in LSTM-RNN model; (c) Observed and predicted TDS correlation in calibration duration in LSTM-RNN model; (d) Observed and predicted TDS correlation in verification duration in LSTM-RNN model.

Table 8. Selected model for predicting TDS and SAR.

Selected models	SAR	TDS
Network	RNN	RNN
Input	Q(t), Q(t-1), P(t),p(t-1)	Q(t) , Q(t-1),Q(t-2) P(t),P(t-1)
Dense layer	2	2
Activation layer	Relu	Relu
Number of neurons	50	100
Optimizer	Rmsprop	Rmsprop
The number of repetitions	1000	5000

3.4. Prediction of TDS and SAR with LSTM-RNN

The neural network model was calibrated for the parameters of sodium adsorption ratio (SAR) and total dissolved solids (TDS) in the base period (2005-2015). The selected model characteristics are presented in Table 8. In this study, observed discharge, rainfall and their monthly delays are chosen for the input of the model. In order to calibrate each of the quality parameters, up to 1000 runs in different models with inputs, networks, activation layer, the number of Dense layer, the number of different neurons were taken. The results of the calibration and validation steps of both parameters are shown in Table 9 and Fig.7. After calibrating and validating the model for the basic period 2005 to 2015, the input data of the next stage including rainfall, temperature and discharge time series and two months delay was used as an input to the LSTM-RNN model to predict TDS and SAR parameters in the next period 2020-2030 (Fig. 8). In the base period, the average, maximum and minimum long-term TDS values are 305, 410 and 78 mg/L, respectively. The results of the TDS forecast for 2020 to 2030 under the RCP4.5 scenario show the values of 295, 410 and 263 mg/L, respectively. The RCP6 results are respectively 302, 410 and 257 mg/L and under the RCP8.5 scenario, are equal to 292, 410 and 257 mg/L. Meanwhile, in the basic period, the average, maximum and minimum long-term SAR values are 0.45, 1.27 and 0.08, respectively. While for the RCP4.5 scenario 0.42, 0.93 and 0.14, and for the RCP6 are 0.44, 0.94 and 0.1 respectively and for the RCP8.5, the values are 0.42, 0.93 and 0.15.

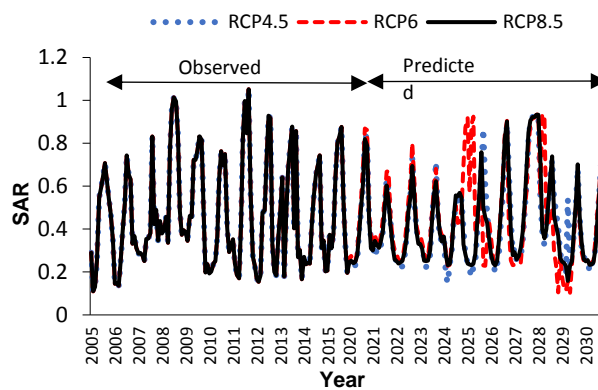


Fig. 8. (a) Predicted TDS in different RCP scenarios; (b) Predicted SAR in different RCP scenarios.

Table 9. LSTM Performance criteria in calibration and verification duration.

Parameters	Calibration			
	R	MAE	RMSE	NSE
TDS	0.95	0.054	0.1	0.69
SAR	0.81	0.57	0.19	0.53
Parameters	Verification			
	R	MAE	RMSE	NSE
TDS	0.98	0.019	0.06	0.61
SAR	0.83	0.25	0.16	0.51

4. Conclusions and remarks

In this study, the output of four climate models of the IPCC Fifth Assessment Report (AR5) under RCP4.5, RCP6 and RCP8.5 scenarios for precipitation and temperature parameters were extracted in the base period and compared with observational climate data, then, the models were evaluated based on error criteria and the observational data. The results indicated that despite of the fine ability of all models in simulation, but the difference in output obtained from each model shows the uncertainty of climate models. The reduction of model uncertainty was done by MOTP method. The monthly rainfall and temperature parameters for future periods 2020-2052 and 2053-2085 were obtained according to the output of the weight combination model. In order to simulate runoff in the basic period 1983-2015, the rainfall-runoff model of IHACRES was calibrated and validated. In order to evaluate and predict the water quality status of Khorramrood river in terms of TDS

and SAR indicators, LSTM –RNN method was used in the Python programming environment. The performance of the artificial neural evaluated and the optimal model predicted TDS and SAR for the future period of 2020-2030. The results of predicting TDS values show that despite the small changes in the average and maximum value of this parameter in the future period compared to the observation period, the minimum value of this parameter has increased sharply. However, the SAR parameter does not show significant changes in these values, and in both parameters, increasing changes are observed in 2024 and 2025. Prediction of river quality parameters in comparison with Baek et al. (2020) and Hu et al. (2019) researches showed that LSTM-RNN method is a suitable method for predicting water quality parameters. In general, in less populated areas, the rate of changes in water quality parameters is less than in populated areas, so the amount of changes in TDS and SAR in Aran station in case of non-industrialization of the area and control of pesticides and observed water right of Anahita dam, in future periods does not increase indiscriminately and does not require structural measures to control, but always non-structural strategies to maintain water quality is essential.

Acknowledgments

The authors would like to thank Regional Water Company and Province Meteorological Administration, Kermanshah, Iran.

References

- Andréassian V., Lerat J., Le Moine N., Perrin C., Neighbors: Nature's own hydrological models, *Journal of Hydrology* 414 (2012) 49–58.
- Ansari-pour A., Jamali B., Ebrahimi K., Assessment of artificial neural network and multi variable regression in predicting water quality parameters (case study: Sefidrood river) Guilan, 10th Iran hydraulic conference, Rasht, Guilan University (2011).
- Asadollahfardi G., Taklifi A., Ghanbari A., Application of artificial neural network to predict TDS in Talkheh Rud river, *Journal of Irrigation and Drainage Engineering* 138 (2011) 363-370.
- Asadollahfardi G., Hemati A., Moradinejad S., Asadollahfardi R., Sodium adsorption ratio (SAR) prediction of the Chalgazi river using artificial neural network (ANN), *Current World Environment* 8 (2013) 169-178.
- Asadollahfardi G., Zangoeei H., Aria S.H., Danesh E., Application of artificial neural networks to predict total dissolved solids at the Karaj dam, *Environmental Quality Management* 26 (2017) 55-72.
- Azamatulla H.M., Deo M.C., Deolalikar P.B., Alternative neural networks to estimate the scour below spillways, *Advanced Engineer Software* 36 (2008) 656–665.
- Azamatulla H.M., A review on application of soft computing methods in water resources engineering A6. In: Yang X.S., Gandomi M.H., Talatahari S., Alavi A.H (eds), *Metaheuristics in water, Geotechnical and Transport Engineering*. Elsevier, Oxford (2013) 41–67.
- Azari M., Moradi H.R., Saghafian B., Faramarzi M., Assessment of hydrological of climate change in Gourganrood river basin, *Journal of Water and Soil (Agricultural sciences and technology)* 27 (2013) 527-547 (In Persian).
- Baek S.S., Pyo J., Chun J.A., Prediction of water level and water quality using a CNN-LSTM combined deep learning approach. *Water* 12 (2020) 3399.
- Bal P.K., Ramachandran A., Geetha R., Bhaskaran B., Thirumurugan P., Indumathi J., Jayanthi N., Climate change projections for Tamil Nadu, India: deriving high resolution climate data by a downscaling approach using PRECIS. *Theoretical and Applied Climatology* 123 (2016) 523–535.
- Burchard-Levine A., Liu S., Vince F., Li M., Ostfeld A., A hybrid evolutionary data driven model for river water quality early warning, *Journal of Environmental Management* 143 (2014) 5–16.
- Burnash R.J.C., Ferral R.L., McGuire R.A.A., Generalized stream flow simulation system: Conceptual modeling for digital computers, Technical Report; U.S. National Weather Service: Sacramento, CA, USA (1973).
- Carlijn van der Sluis., The Integration of climate change in a prioritization method for emerging for risks to drinking water quality, Utrecht University and National Institute for Public Health and the Environment. Master thesis (2019).
- Chang F.J., Chung C.H., Chen P.A., Liu C.W., Coynel A., Vachaud G., Assessment of arsenic concentration in stream water using neuro fuzzy networks with factor analysis, *Science of the Total Environment* 494-495 (2014) 202-210.
- Cordoba G.A.C., Tuhovc'a'k L., Taus' M., Using artificial neural network models to assess water quality in water distribution networks, *Procedia Engineering* 70 (2014) 366–405.
- DÉQUÉ M., Rowell D., Lüthi D., Giorgi F., Christensen J., Rockel B., Jacob D., Kjellstrom E., Castro D., Hurk V., An inter comparison of regional climate simulations for Europe: assessing uncertainties in model projections, *Climatic Change* 81 (2007) 53-70.
- Delpla I., Jung A., Baures E., Clement M., Thomas O., Impacts of climate change on surface water quality in relation to drinking water production, *Environment International* 35 (2009) 1225-1233.
- Diaz-Nieto J., and Wilby R.L., A comparison of statistical downscaling and climate change factor methods: impacts on low flows in the river Thames, United Kingdom, *Climatic Change* 69 (2005) 245-268.
- Eghtetaf M., Dahrazma B., Zarghami M., Saghravani S.F., Impact of climate change on the quantity and quality of surface water resources (case study: Balikhli Chay river), Civil and Architectural Engineering, MSc thesis, Shahrood University (2015) (In Persian).
- Ghavidel S. Z. Z., and Montaseri M., Application of different data-driven methods for the prediction of total dissolved solids in the Zarinerood basin, *Stochastic Environmental Research and Risk Assessment* 28 (2014) 2101-2118.
- Gazzaz N.M., Yusoff M.K., Zaharin Aris A., Juahir H., Ramli M.F., Artificial neural network modeling of the water quality index for Kinta river (Malaysia) using water quality variables as predictors, *Journal of Marine Pollution Bulletin* 64 (2012) 2409-2420.
- Guilbert J., The impacts of climate change on precipitation and hydrology in the northeastern United States. Graduate College Dissertations and Thesis. University of Vermont (2016).
- Hind A., Aldulaimi A., Al-Zuhairi M., Prediction and forecasting of total dissolved solids (TDS) by recurrent neural networks, *Journal of Advanced Research in Dynamical and Control Systems* 10 (2018) 1922-1944
- Hochreiter S., and Schmidhuber J., Long short-term memory, *Neural Computation* 9 (1997) 1735-1780.
- Hosseini N., Johnston J., Lindenschmidt K.E., Impacts of climate change on the water quality of a regulated prairie river, *Water* 9 (2017) 199.
- Hu Z., Zhang Y., Zhao Y., Xie M., Zhong J., Tu Z., Liu J., A water quality prediction method based on the deep LSTM network considering correlation in smart mariculture, *Sensors* 19 (2019) 1-20.
- Jakeman A.J., and Hornberger G.M., How much complexity is warranted in a rainfall-runoff model? *Water Resources Research* 66 (1993) 6637-6646.
- Jiménez Cisneros B. E., Oki T., Arnell N. W., Benito G., Cogley J. G., Döll P., Mwakali S., Freshwater resources. In Field C. B., Barros V.R., Dokken D.J., Mach K.J., Mastrandrea M.D., Bilir T.E., Chatterjee M., Ebi K.L., Estrada Y.O., Genova R.C., Girma B., Kissel E.S., Levy A.N., MacCracken S., Mastrandrea P.R., and White L.L., *Climate change 2014: Impacts, adaptation, and vulnerability. Part A: Global and sectoral aspects. Contribution of working group II to the fifth assessment report of the intergovernmental panel on climate change: 229-269*. Cambridge, UK and New York, NY, USA: Cambridge University Press (2014).
- Kalin L., Isik S., Schoonover J. E., Lockaby B. G., Predicting water quality in unmonitored watersheds using artificial neural networks. *Journal of Environmental Quality* 39 (2010) 1429-1440.
- Maier,H.R., and Dandy G.C., The use of artificial neural networks for the prediction of water quality parameters, *Water Resource Research*,32 (1996) 1013-1022.
- Massah Bavani A.R., Risk assessment of climate change and its impact on water resources, case study: Zayandehrood basin, PhD thesis, Tarbiat Modarres University, Iran (2006) (In Persian).
- Mukundana R., Hoangb L., Geldaa R., Yeoc M., Owensa E., Climate change impact on nutrient loading in a water supply watershed, *Journal of Hydrology* 586 (2020) 1-9.

- Najah A., El-Shafie A., Karim O.A., El-Shafie A.H., Application of artificial neural networks for water quality prediction, *Neural Computing and Applications* 22 (2013) 187-201.
- Nasr M., Zahran H.F., Using of pH as a tool to predict salinity of groundwater for irrigation purpose using artificial neural network, *Egyptian Journal of Aquatic Research* 40 (2014) 111-115.
- Nazaripooaya H., Kardavani P., Farajirad A., Calibration and evaluation of hydrological models, IHACRES and SWAT models in runoff simulation, *Journal of Spatial Analysis Environmental Hazards* 2 (2015) 99-112.
- Nikoo M., Nikoo M., Babahi nejad T., Amiri A., Rostampour gh., Determining water quality along the river with using evolutionary artificial neural networks (case study: Karoon river, shahid abbaspur - arab asad reach), *Journal Of Water Sciences and Engineering* 1 (2011) 45 – 58 (In Persian).
- Noori R., Deng Z., Kiaghadi A., Kachoosangi F.T., How reliable are ANN, ANFIS, and SVM techniques for predicting longitudinal dispersion coefficient in Natural rivers? *Journal of Hydraulic Engineering* 142 (2015) 1-8.
- Noushadi M., Salemi H.R., Ahmadi Zadeh M., Simulation and prediction of some water quality parameters in the Zayanderood river using artificial neural network, *Water and Wastewater* 18 (2008) 49-65 (In Persian).
- Owusu-Boateng G., Adjei V., The potential utilization of grey water for irrigation: A case study on the Kwame Nkrumah University of Science and Technology, Kumasi Campus. *Journal of Applied Research in Water and Wastewater* 1 (2014) 28-34.
- Palani S., Shie-Yui L., Tkalich P., An ANN application for water quality forecasting, *Marine Pollution Bulletin* 56 (2008) 1586-1597.
- Salami E.S., Salari M., Ehteshami M., Bidokhti N.T., Ghadimi H., Application of artificial neural networks and mathematical modeling for the prediction of water quality variables (case study: southwest of Iran), *Desalination and Water Treatment* 57 (2016) 27073-27084.
- Shahkarami N., Detection of climate change and its impact on the trend of water quality in Kamal Saleh dam basin, *Journal of Irrigation and Water Engineering* 8 (2018) 158-171.
- Shin M.J., Eum H.I., Kim C.S., and Jung I.W., Alteration of hydrologic indicators for Korean catchments under CMIP5 climate projections, *Hydrological Processes* 30 (2016) 4517-4542.
- Slaughter A.S., Mantel S.K., Hughes D.A., Water quality management in the context of future climate and development changes: a South African case study, *Journal of Water and Climate Change* 7 (2016) 775-787.
- Sluis CA van der., The integration of climate change in a prioritization method for emerging risks to drinking water quality, *Utrecht University & National Institute for Public Health and the Environment Faculty of Geosciences, Master thesis* (2019).
- Taei Semiromi S., Moradi H.R., Khodaghali M., Evaluation change in Nayshabour Bar river flow under different climate change scenarios, *Human and Environment* 12 (2014) 1-19 (In Persian).
- Tisseuil C1., Vrac M., Grenouillet G., Wade A.J., Gevrey M., Oberdorff T., Grodwohl J.B., Lek S., Strengthening the link between climate, hydrological and species distribution modeling to assess the impacts of climate change on freshwater biodiversity, *Science Total Environment* 424 (2012) 193-201.
- Van Ael E., De Cooman W., Blust R., Bervoets L., Use of a macro invertebrate based biotic index to estimate critical metal concentrations for good ecological water quality, *Chemosphere* 57 116 (2015) 135-144.
- Van Werkhoven K., Wagener T., Reed P., Tang Y., Sensitivity-guided reduction of parametric dimensionality for multi-objective calibration of watershed models, *Advanced Water Resources* 32 (2009) 1154-1169.
- Vörösmarty C., McIntyre P.B., Gessner M.O., Dudgeon D., Prusevich A., Green P., Glidden S.E., Bunn S., Sullivan C.A., Reidy Liermann C., Davies P.M., Global threats to human water security and river biodiversity, *Nature* 467 (2010) 555-561.
- Whitehead P., Wilby R., Battarbee R., Kernan M., Wade A.J., A review of the potential impacts of climate change on surface water quality, *Hydrological Sciences Journal* 54 (2009) 101-123.
- Zare Abyaneh H., Evaluation of multivariate linear regression and artificial neural networks in prediction of water quality parameters, *Journal of Environmental Health Science and Engineering* 16 (2014) 1-5.